10. Tai MH, Wang LL, Wu KL, Chan JY. Increased superoxide anion in rostral ventrolateral medulla contributes to hypertension in spontaneously hypertensive rats via interactions with nitric oxide. *Free Radic Biol Med* 2005; 38:450–462.
11. Chan SH, Tai MH, Li CY, Chan JY. Reduction in molecular synthesis or enzyme activity of superoxide dismutases and catalase contributes to oxidative stress and neurogenic hypertension in spontaneously hypertensive rats. *Free Radic Biol Med* 2006; 40:2028–2039.
12. Oliveira-Sales EB, Nishi EE, Carillo BA, Boim MA, Dolnikoff MS, Bergamaschi CT, Campos RR. Oxidative stress in the sympathetic premotor neurons contributes to sympathetic activation in renovascular hypertension. *Am J Hypertens* 2009; 22:484–492.
13. Oliveira-Sales EB, Colombari DS, Davisson RL, Kasparov S, Hirata AE, Campos RR, Paton JF. Kidney-induced hypertension depends on superoxide signaling in the rostral ventrolateral medulla. *Hypertension* 2010; 56:290–296.
14. Sakai K, Hirooka Y, Matsuo I, Eshima K, Shigematsu H, Shimokawa H, Takeshita A. Overexpression of eNOS in NTS causes hypotension and bradycardia in vivo. *Hypertension* 2000; 36:1023–1028.
15. Hirooka Y, Sakai K, Kishi T, Takeshita A. Adenovirus-mediated gene transfer into the NTS in conscious rats. A new approach to examining the central control of cardiovascular regulation. *Ann N Y Acad Sci* 2001; 940:197–205.
16. Benarroch EE. Paraventricular nucleus, stress response, and cardiovascular disease. *Clin Auton Res* 2005; 15:254–263.
17. Yang Z, Bertram D, Coote JH. The role of glutamate and vasopressin in the excitation of RVL neurones by paraventricular neurones.. *Brain Res* 2001; 908:99–103.
18. Hardy SG. Hypothalamic projections to cardiovascular centers of the medulla. *Brain Res* 2001; 894:233–240.
19. Kawabe T, Chitravanshi VC, Nakamura T, Kawabe K, Sapru HN. Mechanism of heart rate responses elicited by chemical stimulation of the hypothalamic paraventricular nucleus in the rat. *Brain Res* 2009; 1248:115–126.
20. Zimmerman MC, Lazartigues E, Lang JA, Sinnayah P, Ahmad IM, Spitz DR, Davisson RL. Superoxide mediates the actions of angiotensin II in the central nervous system. *Circ Res* 2002; 91:1038–1045.
21. McKinley MJ, Albiston AL, Allen AM, Mathai ML, May CN, McAllen RM, *et al.* The brain renin-angiotensin system: location and physiological roles. *Int J Biochem Cell Biol* 2003; 35:901–918.
22. Hirooka Y, Sagara Y, Kishi T, Sunagawa K. Oxidative stress and central cardiovascular regulation: pathogenesis of hypertension and therapeutic aspects. *Circ J* 2010; 74:827–835.
23. Li YF, Roy SK, Channon KM, Zucker IH, Patel KP. Effect of in vivo gene transfer of nNOS in the PVN on renal nerve discharge in rats. *Am J Physiol Heart Circ Physiol* 2002; 282:H594–H601.
24. Northcott CA, Watts S, Chen Y, Morris M, Chen A, Haywood JR. Adenoviral inhibition of AT1a receptors in the paraventricular nucleus inhibits acute increases in mean arterial blood pressure in the rat. *Am J Physiol Regul Integr Comp Physiol* 2010; 299:R1202–R1211.
25. Kishi T, Hirooka Y, Sakai K, Shigematsu H, Shimokawa H, Takeshita A. Overexpression of eNOS in the RVLM causes hypotension and bradycardia via GABA release. *Hypertension* 2001; 38:896–901.
26. Nozoe M, Hirooka Y, Koga Y, Araki S, Konno S, Kishi T, *et al.* Mitochondria-derived reactive oxygen species mediate sympathoexcitation induced by angiotensin II in the rostral ventrolateral medulla. *J Hypertens* 2008; 26:2176–2184.
27. Zwacka RM, Dudus L, Epperly MW, Greenberger JS, Engelhardt JF. Redox gene therapy protects human IB-3 lung epithelial cells against ionizing radiation-induced apoptosis. *Hum Gene Ther* 1998; 9:1381–1386.
28. Zwacka RM, Zhou W, Zhang Y, Darby CJ, Dudus L, Halldorson J, *et al.* Redox gene therapy for ischemia/reperfusion injury of the liver reduces AP1 and NF-kappaB activation. *Nat Med* 1998; 4:698–704.
29. Kishi T, Hirooka Y, Kimura Y, Sakai K, Ito K, Shimokawa H, Takeshita A. Overexpression of eNOS in RVLM improves impaired baroreflex control of heart rate in SHRSP. Rostral ventrolateral medulla. Stroke-prone spontaneously hypertensive rats. *Hypertension* 2003; 41:255–260.
30. Chapleau MW, Sabharwal R. Methods of assessing vagus nerve activity and reflexes. *Heart Fail Rev* 2011; 16:109–127.
31. Tagawa T, Dampney RA. AT1 receptors mediate excitatory inputs to rostral ventrolateral medulla pressor neurons from hypothalamus. *Hypertension* 1999; 34:1301–1307.
32. Yang Z, Han D, Coote JH. Cardiac sympatho-excitatory action of PVN-spinal oxytocin neurones. *Auton Neurosci* 2009; 147:80–85.
33. Chen QH, Haywood JR, Toney GM. Sympathoexcitation by PVN-injected bicuculline requires activation of excitatory amino acid receptors. *Hypertension* 2003; 42:725–731.
34. Li YF, Jackson KL, Stern JE, Rabeler B, Patel KP. Interaction between glutamate and GABA systems in the integration of sympathetic outflow by the paraventricular nucleus of the hypothalamus. *Am J Physiol Heart Circ Physiol* 2006; 291:H2847–H2856.
35. Kannan H, Niijima A, Yamashita H. Effects of stimulation of the hypothalamic paraventricular nucleus on blood pressure and renal sympathetic nerve activity. *Brain Res Bull* 1988; 20:779–783.
36. Yamashita H, Kannan H, Kasai M, Osaka T. Decrease in blood pressure by stimulation of the rat hypothalamic paraventricular nucleus with L-glutamate or weak current. *J Auton Nerv Syst* 1987; 19:229–234.
37. Allen AM. Inhibition of the hypothalamic paraventricular nucleus in spontaneously hypertensive rats dramatically reduces sympathetic vasomotor tone. *Hypertension* 2002; 39:275–280.
38. Kagiyama S, Tsuchihashi T, Abe I, Matsumura K, Fujishima M. Antisense inhibition of angiotensinogen attenuates vasopressin release in the paraventricular hypothalamic nucleus of spontaneously hypertensive rats. *Brain Res* 1999; 829:120–124.
39. Chen QH, Toney GM. AT1-receptor blockade in the hypothalamic PVN reduces central hyperosmolality-induced renal sympathoexcitation. *Am J Physiol Regul Integr Comp Physiol* 2001; 281:R1844–R1853.
40. Han Y, Zhang Y, Wang HJ, Gao XY, Wang W, Zhu GQ. Reactive oxygen species in paraventricular nucleus modulates cardiac sympathetic afferent reflex in rats. *Brain Res* 2005; 1058:82–90.

Reviewers' Summary Evaluations

Referee 1

Nishihara *et al.*, tested the hypothesis of a respective role of oxidative stress in the PVN and RVLM in the regulation of BP in SHR rats. They demonstrated for the first time that while oxidative stress in the RVLM affects both BP and HR, oxidative stress in the PVN modulates HR only. A cumulative effect of oxidative stress in the PVN and RVLM, on the control of HR was also reported. This study is the first to provide good evidence for a different contribution of oxidative stress in the PVN and RVLM in the control of BP and HR.

Referee 2

MnSOD transfection into the PVN of SHR reduces HR but not arterial pressure as it does when transfected into the RVLM. The data indicate that a reduced abundance of ROS in the PVN and RVLM of SHR has differential effects on the regulation of cardiovascular function via the autonomic nervous system. It remains to be clarified if the effects of MnSOD transfection reported here are due to reductions in ROS formation and abundance in neurons, glia or both.

Inhibition of Oxidative Stress in Rostral Ventrolateral Medulla Improves Impaired Baroreflex Sensitivity in Stroke-Prone Spontaneously Hypertensive Rats

Kiyohiro OGAWA,[1] MD, Yoshitaka HIROOKA,[2] MD, Keisuke SHINOHARA,[1] MD, Takuya KISHI,[3] MD, *and* Kenji SUNAGAWA,[1] MD

SUMMARY

Reactive oxygen species (ROS) in rostral ventrolateral medulla (RVLM) of brainstem contribute to sympathoexcitation and are critically involved in the pathogenesis of hypertension. Baroreflex sensitivity (BRS) is a valuable prognostic parameter of the autonomic nervous system, and is impaired in hypertension. The aim of the present study was to determine whether or not a chronic reduction of ROS in the RVLM improves impaired BRS in hypertensive rats. We transfected adenovirus vectors encoding either manganese superoxide dismutase (AdMnSOD) or β-galactosidase (AdLacZ) into the RVLM of stroke-prone spontaneously hypertensive rats (SHRSP). We measured BRS using the spontaneous sequence method. BRS was significantly lower in SHRSPs than in Wistar-Kyoto rats. In the AdMnSOD-transfected SHRSP, blood pressure, heart rate, and sympathetic nervous system activation were significantly decreased from day 5 after the gene transfer. BRS in the AdMnSOD-transfected SHRSP was significantly increased from day 4 after the gene transfer with the reduction of ROS in the RVLM. Furthermore, in the AdMnSOD-transfected SHRSP, intravenous infusion of atropine dramatically decreased BRS. In contrast, in the AdLacZ-transfected SHRSP, atropine did not decrease BRS. These results suggest that chronic reduction of ROS in the local RVLM improves the impaired BRS in SHRSP through inhibition of the sympathetic component. (Int Heart J 2012; 53: 193-198)

Key words: Baroreflex sensitivity, Reactive oxygen species, Brain, Sympathetic nervous system, Hypertension

A change in arterial blood pressure (BP), such as that resulting from postural change, is detected by baroreceptors, and the afferent nerves provide the information to the central nervous system.[1,2] The arterial baroreflex regulated by the central nervous system acts to oppose the increase in BP by inhibiting sympathetic activity, causing vasodilation and slowing heart rate (HR) in the short-term.[1,2] Previous reports have suggested that baroreflex sensitivity (BRS) is impaired in cardiovascular diseases such as hypertension,[3-6] heart failure,[7,8] and myocardial infarction.[9] It has been suggested that BP variability, which is a cardiovascular risk factor, contributes to end-organ damage.[10-12] The assessment of BRS has been considered to be the established tool for the evaluation of autonomic control of the cardiovascular system.[9,13] Classically, BRS has been evaluated by the drug-induced Oxford method.[14] However, pharmacological assessment of BRS is difficult to determine repeatedly in humans, but can be done in acute experiments with anesthetized animals. Recently, the spontaneous sequence method has proved to be a reliable and noninvasive method for assessing BRS, and the assessment of BRS can now be performed repeatedly in humans and animals in a conscious state.[4,15]

The rostral ventrolateral medulla (RVLM) is the vasomotor center that determines basal sympathetic nervous system (SNS) activation, and is responsible for maintaining sympathetic out flow.[1,2] The RVLM receives input from multiple areas of the brain and determines the SNS activation to maintain the stability of BP and HR. Previously, we reported that nitric oxide in the RVLM caused sympathoinhibition and improved impaired BRS in hypertensive rats.[5] Furthermore, we have demonstrated that the reduction of reactive oxygen species (ROS) induced by manganese superoxide dismutase (MnSOD) gene transfer into the bilateral RVLM causes sympathoinhibition in hypertensive rats. These results suggest that ROS in the RVLM causes sympathoexcitation in hypertensive rats.[16] Therefore, we believe that ROS in the RVLM might impair BRS in hypertensive rats. However, it has not been demonstrated whether the chronic reduction of ROS in the RVLM could improve the impaired BRS in hypertensive rats. The aim of the present study was to determine whether or not the chronic reduction of ROS via overexpression of MnSOD in the local RVLM of conscious hypertensive rats improves the impaired BRS.

From the Departments of [1] Cardiovascular Medicine, [2] Advanced Cardiovascular Regulation and Therapeutics, and [3] Advanced Therapeutics for Cardiovascular Diseases, Kyushu University Graduate School of Medical Science, Fukuoka, Japan.

This study was supported by a Grant-in-Aid for Scientific Research from the Japan Society for the Promotion of Science (B193290231) and, in part, a Kimura Memorial Foundation Research Grant.

Address for correspondence: Yoshitaka Hirooka, MD, Department of Advanced Cardiovascular Regulation and Therapeutics, Kyushu University Graduate School of Medical Sciences, 3-1-1 Maidashi, Higashi-ku, Fukuoka, Fukuoka 812-8582, Japan.

Received for publication March 9, 2012.

Accepted March 29, 2012.

METHODS

This study was reviewed and approved by the Committee on the Ethics of Animal Experiments of Kyushu University Graduate School of Medical Sciences and was conducted according to the Guidelines for Animal Experiments of Kyushu University.

Animals: Male stroke-prone spontaneously hypertensive rats (SHRSP) and age-matched Wistar-Kyoto (WKY) rats (12 to 14 weeks old) fed standard feed were used. The rats were purchased from SLC Japan (Hamamatsu, Japan).

Radio-telemetry monitoring of BP and HR: A UA-10 telemetry system (Data Science International) was used to measure BP and HR, as described previously.[17-20] The rats were allowed to recover from implantation of the telemetry system for 7-8 days before starting the protocol. HR was derived from the BP interval using a PowerLab (AD Instruments Inc.) data acquisition system.

***In vivo* gene transfer of MnSOD into the RVLM:** Adenovirus vectors encoding either bacterial β-galactosidase gene (AdLacZ) or MnSOD gene (AdMnSOD) were transfected into the bilateral RVLM (SHRSP transfected with AdMnSOD [AdMnSOD-transfected SHRSP], SHRSPs transfected with AdLacZ [AdLacZ-transfected SHRSPs], and WKY rats transfected with AdMnSOD [AdMnSOD-transfected WKY rats]). The method of transfection was described previously.[16,18] AdMnSOD and AdLacZ were constructed in the Gene Transfer Core Laboratory at the University of Iowa, Iowa City.[21] Procedures for microinjection of the vectors into the RVLM have been described previously.[18]

Analysis of gene overexpression for MnSOD: To confirm the local overexpression of MnSOD in the RVLM, Western blotting analysis for MnSOD protein in the RVLM or cortex tissues of AdMnSOD-transfected SHRSP was performed at day 0, 7, and 21 after the gene transfer. In the Western blotting analysis for MnSOD protein, mouse IgG monoclonal antibody to MnSOD (1:1000, Transduction Laboratories) was used as described previously.[16]

Measurement of ROS in the RVLM: To confirm ROS activity, thiobarbituric acid-reactive substance (TBARS) levels in the RVLM tissue were measured at day 7 after the gene transfer as described previously.[16]

Measurement of urinary norepinephrine excretion: Twenty-four hour urinary norepinephrine excretion was measured before and at day 7 after the gene transfer as described previously as a noninvasive indicator of SNS activation.[18,22,23]

Measurement of conscious BRS by spontaneous sequence method: BRS was measured using a spontaneous sequence method. The subjects were given a 10-minute rest period to allow for stabilization of BP or HR. To analyze approximately 5 minutes of hemodynamic recordings from the telemetry system, we selected all sequences of three or more successive heart beats in which there was a concordant increase (Up sequence) or decrease (Down sequence) in arterial systolic BP and peak-to-peak systolic BP interval change. Linear regression was applied to each sequence, and an average regression slope was calculated for the sequences. This slope represents the cardiac BRS. The threshold values for including beat-to-beat systolic BP and its interval changes in a sequence were set at 1 mmHg and 2 milliseconds, respectively.

Effects of autonomic blockade on BRS: Autonomic nervous system blockade was performed to determine the sympathetic and parasympathetic components. Intravenous injection via a tail vein was performed under light pentobarbital anesthesia. Metoprolol bitartrate (dominant to parasympathetic component) (a selective β_1-receptor blocker, 0.2 mg/kg) or atropine methyl bromide (dominant to sympathetic component) (0.02 mg/kg) was injected intravenously at day 7 after the gene transfer, and then the changes in HR and BRS in each group were measured.

Statistical analysis: All data are expressed as the mean ± SEM. ANOVA was used to compare the TBARS level, and changes in mean blood pressure, heart rate, and BRS. An unpaired t test was used to compare the expression of MnSOD determined by Western blotting analysis and urinary norepinephrine excretion. Differences were considered to be statistically significant at a P value of < 0.05.

RESULTS

Analysis of gene expression of MnSOD: Western blotting anal-

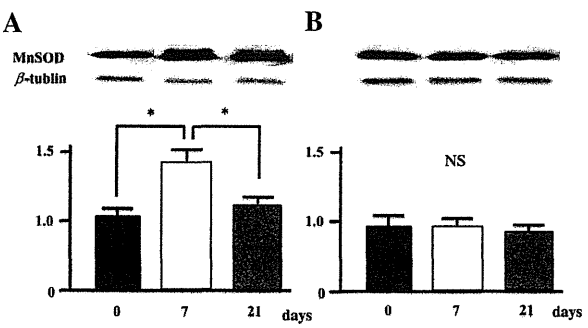

Figure 1. Western blot analysis demonstrating the expression of MnSOD protein in the RVLM (**A**) or cortex (**B**) in AdMnSOD-transfected SHRSP before (day 0) and on day 7 and day 21 after the gene transfer. MnSOD indicates manganese superoxide dismutase. $^*P < 0.01$, $n = 5$ for each group.

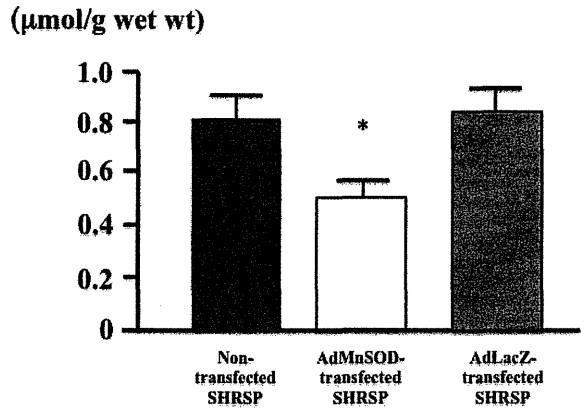

Figure 2. TBARS level in RVLM tissue from nontransfected SHRSPs, AdMnSOD-transfected SHRSP, and AdLacZ-transfected SHRSP. The RVLM tissues from AdMnSOD-transfected and AdLacZ-transfected SHRSP were obtained at day 7 after the gene transfer. $^*P < 0.01$ versus nontransfected SHRSP, $n = 5$ for each group.

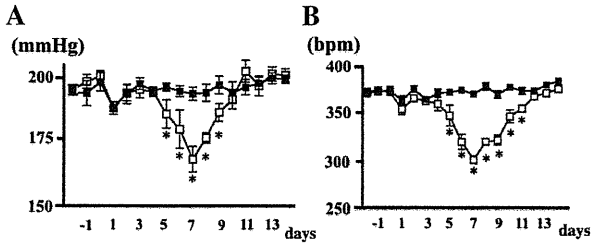

Figure 3. A: Time course of changes in MAP (**A**, in mmHg) and HR (**B**, in beats per minute) in AdMnSOD-transfected SHRSP (open square) and AdLacZ-transfected SHRSP (close square). $^{*}P < 0.05$ versus values of AdLacZ-transfected SHRSP group, $n = 5$ for each group.

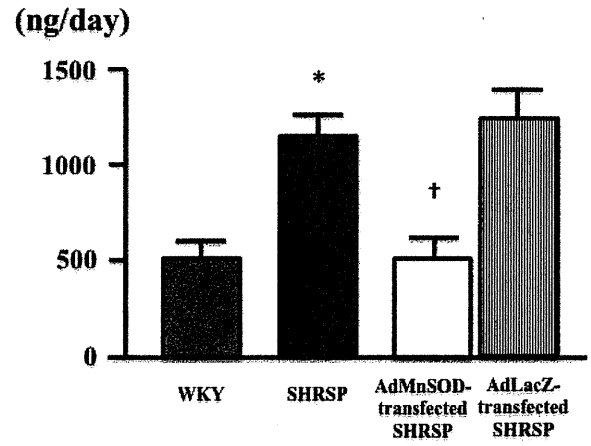

Figure 4. 24-hour urinary norepinephrine excretion in WKY rats (AdMnSOD-transfected WKY rats before the gene transfer), SHRSP (AdMnSOD-transfected SHRSP before the gene transfer), AdMnSOD-transfected SHRSP at day 7 after the gene transfer, and AdLacZ-transfected SHRSP at day 7 after the gene transfer. $^{*}P < 0.01$ in SHRSP versus WKY rats, $n = 5$ for each group. $^{\dagger}P < 0.05$ in AdMnSOD-transfected SHRSP versus AdLacZ-transfected SHRSP, $n = 5$ for each group. WKY indicates Wistar-Kyoto rats; SHRSP, stroke-prone spontaneously hypertensive rats; AdMnSOD, adenovirus vectors encoding manganese superoxide dismutase; and AdLacZ, adenovirus vectors encoding the bacterial β-galactosidase gene.

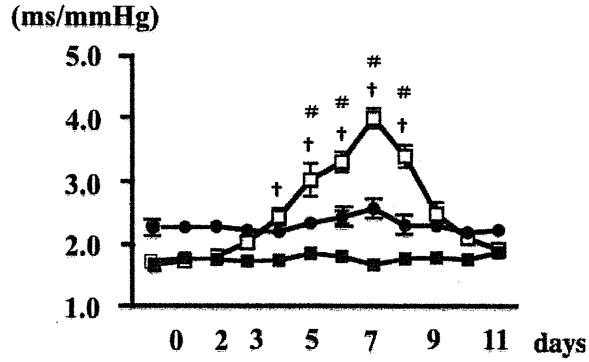

Figure 5. Time course of BRS (in ms/mmHg) in AdMnSOD-transfected SHRSP (open square), AdLacZ-transfected SHRSP (close square), and AdMnSOD-transfected WKY rats (close circle). $^{\dagger}P < 0.01$ in AdMnSOD-transfected SHRSP versus value of AdLacZ-transfected SHRSP, $n = 5$ for each group. $^{\#}P < 0.05$ in AdMnSOD-transfected SHRSP versus value of AdMnSOD-transfected WKY rats, $n = 5$ for each group. ms indicates milliseconds.

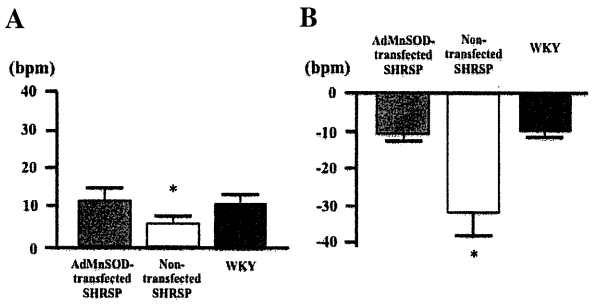

Figure 6. Changes in HR (in beats per minute) after blockade of autonomic nervous system in WKY rats, AdMnSOD-transfected SHRSP, and nontransfected SHRSP. **A:** Changes in HR after intravenous injection of atropine. **B:** Changes in HR after intravenous injection of metoprolol. $^{*}P < 0.05$ versus AdMnSOD-transfected SHRSP, $n = 4$ for each group. WKY indicates Wistar-Kyoto rats; SHRSP, stroke-prone spontaneously hypertensive rats; AdMnSOD, adenovirus vectors encoding manganese superoxide dismutase; AdLacZ, adenovirus vectors encoding the bacterial β-galactosidase gene; and bpm, beats per minute.

ysis showed that the expression of MnSOD protein was significantly increased in tissue from the RVLM of AdMnSOD-transfected SHRSP at day 7 after the gene transfer (Figure 1). The expression of MnSOD protein in RVLM was decreased at day 21 after the gene transfer (Figure 1). These changes in expression were not seen in cortex tissue.

TBARS levels in RVLM tissue: TBARS levels were significantly lower in AdMnSOD-transfected SHRSP than in nontransfected SHRSP or AdLacZ-transfected SHRSP (Figure 2).

Mean BP, HR, and urinary norepinephrine excretion: Figure 3 shows the time courses in mean BP (A) and HR (B) in AdMnSOD-transfected and AdLacZ-transfected SHRSP. Mean BP and HR decreased significantly between day 5 to 9 or 11 after the gene transfer in AdMnSOD-transfected SHRSP, but were not seen in AdLacZ-transfected SHRSP. Twenty-four hour urinary norepinephrine excretion was significantly higher in AdMnSOD-transfected SHRSP than in AdMnSOD-transfected WKY rats before the gene transfer (Figure 4). At day 7 after the gene transfer, urinary norepinephrine excretion was significantly decreased in AdMnSOD-transfected SHRSP (Figure 4). In contrast, these changes were not observed in AdLacZ-transfected SHRSP (Figure 4).

Effect of overexpression of MnSOD in RVLM of SHRSPs on BRS: BRS was significantly lower in AdMnSOD-transfected SHRSP than in AdMnSOD-transfected WKY rats before the gene transfer (Figure 5). In contrast, BRS was significantly increased in AdMnSOD-transfected SHRSP to a greater extent than in AdLacZ-transfected SHRSP (Figure 5). BRS was slightly increased at day 3 after the gene transfer in AdMnSOD-transfected SHRSP, and was significantly higher at day 4 after the gene transfer in AdMnSOD-transfected SHRSP than in AdLacZ-transfected SHRSP (Figure 5). The peak value was at day 7 after the gene transfer, and the peak value of BRS was significantly higher in AdMnSOD-transfected SHRSP than in AdMnSOD-transfected WKY rats (Figure 5).

Effect of autonomic blockade on HR and BRS: Blockade of

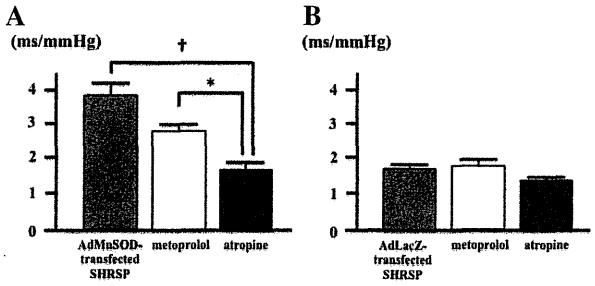

Figure 7. Changes in BRS (in ms/mmHg) after blockade of autonomic nervous system in AdMnSOD-transfected SHRSP (**A**) and AdLacZ-transfected SHRSP (**B**). $^{\dagger}P < 0.01$ in atropine versus AdMnSOD-transfected SHRSP. $^{*}P < 0.01$ in atropine versus metoprolol. SHRSP indicates stroke-prone spontaneously hypertensive rats; AdMnSOD, adenovirus vectors encoding manganese superoxide dismutase; AdLacZ, adenovirus vectors encoding the bacterial β-galactosidase gene; and ms, milliseconds.

the parasympathetic component via systemic infusion of atropine significantly increased HR in AdMnSOD-transfected SHRSP to a greater extent than in non-transfected SHRSP (Figure 6A). Blockade of the sympathetic component via systemic infusion of metoprolol significantly decreased HR in non-transfected SHRSP to a greater extent than in AdMnSOD-transfected SHRSP (Figure 6B). In AdMnSOD-transfected SHRSP, atropine significantly decreased BRS to a greater extent than in metoprolol (Figure 7A). However, in AdLacZ-transfected SHRSP, neither atropine nor metoprolol changed BRS (Figure 7B).

Discussion

The new findings of the present study are that the chronic reduction of ROS induced by overexpression of MnSOD in the RVLM improves impaired BRS in SHRSP through inhibition of the sympathetic component, and that the time course of the change in BRS caused by overexpression of MnSOD in the RVLM of SHRSP is similar to that of the SNS activation. These results indicate that ROS in the RVLM of SHRSP impairs BRS with SNS activation.

We have already demonstrated that ROS in the RVLM contributes to SNS activation,[16] and that NO in the RVLM decreases the SNS activation and improves the impaired BRS in SHRSP.[5] In the present study, we demonstrated that ROS in the RVLM of SHRSP impaired BRS due to activation of the sympathetic component, and that the impaired BRS was improved at almost the same time as the sympathoinhibition. Other reports suggested that intracerebroventricular infusion of exogenous angiotensin II impaired BRS with increased ROS in the RVLM, and that the reduction of ROS in the brain by exercise training or central infusion of simvastatin contributed to the improvement of impaired BRS in cardiovascular diseases.[24-26] These previous reports support the results obtained in the present study. Furthermore, other reports have indicated that electric stimulation of baroreceptors decreased BP, HR and SNS activation,[27,28] and that BRS was improved during baroreceptor stimulation. Interestingly, oral administration of atorvastatin reduced oxidative stress in the RVLM and improved the impaired BRS in SHRSP without sympathoinhibition.[17] We believe that the reduction of ROS in the RVLM improves the impaired BRS in close correlation with sympathoinhibition in SHRSP.

In the present study, the reduction of ROS in the RVLM via overexpression of MnSOD contributed to inhibition of the sympathetic component. These results are compatible with those of our previous study in which the production of NO in the RVLM via overexpression of endothelial NO synthase improved the BRS with inhibition of the sympathetic component.[5,23] Previous reports have demonstrated that a predominant sympathetic component caused impaired BRS.[5,24] In the RVLM, the increase in ROS and decrease in NO resulted in SNS in SHRSP.[18,23] We believe that a reduction in ROS and/or production of NO in the RVLM improved the impaired BRS, probably due to the sympathoinhibition in SHRSP.

Impairment of BRS is considered to be the marker of the risk of mortality or a cardiovascular event in hypertension,[29] heart failure,[9] and ischemic heart diseases.[30] The ATRAMI study demonstrated the prognostic importance of parasympathetic activity as a strong predictor of postmyocardial infarction cardiac mortality.[9] However, cardiovascular events or sudden death occur most frequently toward the end of the night, which coincides with a period when sympathetic activity, BP, and HR change suddenly.[31] Previous reports also have suggested that several antihypertensive agents improved the impaired BRS in hypertension.[5,32,33] Because several antihypertensive drugs, such as calcium channel blockers, have an effect on refractory SNS activation,[34] antihypertensive drugs with sympathoinhibition are preferable for the treatment of hypertension.[33,35] Moreover, because the improvement of BRS contributes to long-term mortality in cardiovascular diseases,[36] antihypertensive agents that improve BRS and possess sympathoinhibition are preferable. In the present study and our previous studies, we have demonstrated that the reduction of ROS in the RVLM causes sympathoinhibition and improvement of BRS in SHRSP.[16,17,22] It is possible that antihypertensive agents with sympathoinhibition and that improve BRS via reduction of oxidative stress in the RVLM might be the most preferable for the treatment of hypertension, because such agents should improve long-term mortality in cardiovascular diseases.

Several questions remain unsolved in the present study. First, the reason why the BRS of AdMnSOD-transfected SHRSP exceeded that of WKY rats could not be clearly elucidated. Second, we used only SHRSP as a hypertensive rat model in the present study. Oxidative stress in the brain was suggested to contribute to SNS activation in other hypertensive models,[37-40] and BRS was impaired in other hypertensive models.[41,42] Thus, it is possible that the results obtained in the present study might be common in hypertensive models. Further studies are needed to determine these issues. Finally, we did not clarify the relationship between BRS and SNS activation in the present study. Recently, we reported that MnSOD-regulated ROS in the RVLM enhanced glutamatergic excitatory inputs and attenuated gamma amino butyric acid (GABA)-mediated inhibitory inputs to the RVLM.[43] Glutamate and GABA in the RVLM are key mediators of baroreflex control.[1,2,5,18] We speculate that these mechanisms could contribute to the improvement of baroreceptor function and sympathoinhibition via overexpression of MnSOD in the RVLM in hypertensive rats.

Conclusions: The present results suggest that a reduction in ROS via overexpression of MnSOD in the RVLM improves the impaired BRS in SHRSP through the inhibition of the sympathetic component. These results indicate that ROS in the RVLM of SHRSP impairs BRS with sympathoexcitation, and that ROS in the RVLM should be the target of treatment for cardiovascular diseases.

REFERENCES

1. Dampney RA. Functional organization of central pathways regulating the cardiovascular system. Physiol Rev 1994; 74: 323-64. (Review)
2. Guyenet PG. The sympathetic control of blood pressure. Nat Rev Neurosci 2006; 7: 335-46. (Review)
3. Mancia G, Ludbrook J, Ferrari A, Gregorini L, Zanchetti A. Baroreceptor reflexes in human hypertension. Circ Res 1978; 43: 170-7.
4. Parati G, Di Rienzo M, Bertinieri G, *et al.* Evaluation of the baroreceptor-heart rate reflex by 24-hour intra-arterial blood pressure monitoring in humans. Hypertension 1988; 12: 214-22.
5. Kishi T, Hirooka Y, Kimura Y, *et al.* Overexpression of eNOS in RVLM improves impaired baroreflex control of heart rate in SHR-SP. Rostral ventrolateral medulla. Stroke-prone spontaneously hypertensive rats. Hypertension 2003; 41: 255-60.
6. Hesse C, Charkoudian N, Liu Z, Joyner MJ, Eisenach JH. Baroreflex sensitivity inversely correlates with ambulatory blood pressure in healthy normotensive humans. Hypertension 2007; 50: 41-6.
7. Davies LC, Francis D, Jurak P, Kara T, Piepoli M, Coats AJ. Reproducibility of methods for assessing baroreflex sensitivity in normal controls and in patients with chronic heart failure. Clin Sci (Lond) 1999; 97: 515-22.
8. Mortara A, La Rovere MT, Pinna GD, *et al.* Arterial baroreflex modulation of heart rate in chronic heart failure: clinical and hemodynamic correlates and prognostic implications. Circulation 1997; 96: 3450-8.
9. La Rovere MT, Bigger JT Jr, Marcus FI, Mortara A, Schwartz PJ. Baroreflex sensitivity and heart-rate variability in prediction of total cardiac mortality after myocardial infarction. ATRAMI (Autonomic Tone and Reflexes After Myocardial Infarction) Investigators. Lancet 1998; 351: 478-84.
10. Shan ZZ, Dai SM, Su DF. Relationship between baroreceptor reflex function and end-organ damage in spontaneously hypertensive rats. Am J Physiol Heart Circ Physiol 1999; 277: H1200-6.
11. Miao CY, Su DF. The importance of blood pressure variability in rat aortic and left ventricular hypertrophy produced by sinoaortic denervation. J Hypertens 2002; 20: 1865-72.
12. Tatasciore A, Renda G, Zimarino M, *et al.* Awake systolic blood pressure variability correlates with target-organ damage in hypertensive subjects. Hypertension 2007; 50: 325-32.
13. Billman GE, Schwartz PJ, Stone HL. Baroreceptor reflex control of heart rate: a predictor of sudden cardiac death. Circulation 1982; 66: 874-80.
14. Smyth HS, Sleight P, Pickering GW. Reflex regulation of arterial pressure during sleep in man. A quantitative method of assessing baroreflex sensitivity. Circ Res 1969; 24: 109-21.
15. Parlow J, Viale JP, Annat G, Hughson R, Quintin L. Spontaneous cardiac baroreflex in humans. Comparison with drug-induced responses. Hypertension 1995; 25: 1058-68.
16. Kishi T, Hirooka Y, Kimura Y, Ito K, Shimokawa H, Takeshita A. Increased reactive oxygen species in rostral ventrolateral medulla contribute to neural mechanisms of hypertension in stroke-prone spontaneously hypertensive rats. Circulation 2004; 109: 2357-62.
17. Kishi T, Hirooka Y, Konno S, Sunagawa K. Atorvastatin improves the impaired baroreflex sensitivity via anti-oxidant effect in the rostral ventrolateral medulla of SHRSP. Clin Exp Hypertens 2009; 31: 698-704.
18. Kishi T, Hirooka Y, Sakai K, Shigematsu H, Shimokawa H, Takeshita A. Overexpression of eNOS in the RVLM causes hypotension and bradycardia via GABA release. Hypertension 2001; 38: 896-901.
19. Sakai K, Hirooka Y, Matsuo I, *et al.* Overexpression of eNOS in NTS causes hypotension and bradycardia in vivo. Hypertension 2000; 36: 1023-8.
20. Hirooka Y, Sakai K, Kishi T, Takeshita A. Adenovirus-mediated gene transfer into the NTS in conscious rats. A new approach to examining the central control of cardiovascular regulation. Ann N Y Acad Sci 2001; 940: 197-205.
21. Zwacka RM, Zhou W, Zhang Y, *et al.* Redox gene therapy for ischemia/reperfusion injury of the liver reduces AP1 and NF-kappaB activation. Nat Med 1998; 4: 698-704.
22. Kishi T, Hirooka Y, Konno S, Ogawa K, Sunagawa K. Angiotensin II type 1 receptor-activated caspase-3 through ras/mitogen-activated protein kinase/extracellular signal-regulated kinase in the rostral ventrolateral medulla is involved in sympathoexcitation in stroke-prone spontaneously hypertensive rats. Hypertension 2010; 55: 291-7.
23. Kishi T, Hirooka Y, Ito K, Sakai K, Shimokawa H, Takeshita A. Cardiovascular effects of overexpression of endothelial nitric oxide synthase in the rostral ventrolateral medulla in stroke-prone spontaneously hypertensive rats. Hypertension 2002; 39: 264-8.
24. Gao L, Wang W, Li YL, *et al.* Sympathoexcitation by central ANG II: roles for AT1 receptor upregulation and NAD(P)H oxidase in RVLM. Am J Physiol Heart Circ Physiol 2005; 288: H2271-9.
25. Gao L, Wang W, Li YL, *et al.* Simvastatin therapy normalizes sympathetic neural control in experimental heart failure: roles of angiotensin II type 1 receptors and NAD(P)H oxidase. Circulation 2005; 112: 1763-70.
26. Pan YX, Gao L, Wang WZ, *et al.* Exercise training prevents arterial baroreflex dysfunction in rats treated with central angiotensin II. Hypertension 2007; 49: 519-27.
27. Lohmeier TE, Irwin ED, Rossing MA, Serdar DJ, Kieval RS. Prolonged activation of the baroreflex produces sustained hypotension. Hypertension 2004; 43: 306-11.
28. Heusser K, Tank J, Engeli S, *et al.* Carotid baroreceptor stimulation, sympathetic activity, baroreflex function, and blood pressure in hypertensive patients. Hypertension 2010; 55: 619-26.
29. Ormezzano O, Cracowski JL, Quesada JL, Pierre H, Mallion JM, Baguet JP. EVAluation of the prognostic value of BARoreflex sensitivity in hypertensive patients: the EVABAR study. J Hypertens 2008; 26: 1373-8.
30. Katsube Y, Saro H, Naka M, *et al.* Decreased baroreflex sensitivity in patients with stable coronary artery disease is correlated with the severity of coronary narrowing. Am J Cardiol 1996; 78: 1007-10.
31. Somers V, Dyken ME, Mark AL, Abboud FM. Sympathetic-nerve activity during sleep in normal subjects. N Engl J Med 1993; 328: 303-7.
32. Munakata M, Aihara A, Nunokawa T, *et al.* The influence of one-year treatment by angiotensin converting enzyme inhibitor on baroreflex sensitivity and flow-mediated vasodilation of the brachial artery in essential hypertension--comparison with calcium channel blockers. Clin Exp Hypertens 2003; 25: 169-81.
33. Kishi T, Hirooka Y, Konno S, Sunagawa K. Cilnidipine inhibits the sympathetic nerve activity and improves baroreflex sensitivity in patients with hypertension. Clin Exp Hypertens 2009; 31: 241-9.
34. Lindqvist M, Kahan T, Melcher A, Ekholm M, Hjemdahl P. Long-term calcium antagonist treatment of human hypertension with mibefradil or amlodipine increases sympathetic nerve activity. J Hypertens 2007; 25: 169-75.
35. Konno S, Hirooka Y, Araki S, Koga Y, Kishi T, Sunagawa K. Azelnidipine decreases sympathetic nerve activity via antioxidant effect in the rostral ventrolateral medulla of stroke-prone spontaneously hypertensive rats. J Cardiovasc Pharmacol 2008; 52: 555-60.
36. Gao L, Wang W, Liu D, Zucker IH. Exercise training normalizes sympathetic outflow by central antioxidant mechanisms in rabbits

with pacing-induced chronic heart failure. Circulation 2007; 115: 3095-102.
37. Zimmerman MC, Lazartigues E, Sharma RV, Davisson RL. Hypertension caused by angiotensin II infusion involves increased superoxide production in the central nervous system. Circ Res 2004; 95: 210-6.
38. Oliveira-Sales EB, Nishi EE, Carillo BA, *et al.* Oxidative stress in the sympathetic premotor neurons contributes to sympathetic activation in renovascular hypertension. Am J Hypertens 2009; 22: 484-92.
39. Fujita M, Ando K, Nagae A, Fujita T. Sympathoexcitation by oxidative stress in the brain mediates arterial pressure elevation in salt-sensitive hypertension. Hypertension 2007; 50: 360-7.
40. Oliveira-Sales EB, Dugaich AP, Carillo BA, *et al.* Oxidative stress contributes to renovascular hypertension. Am J Hypertens 2008; 21: 98-104.
41. Gao SA, Johansson M, Rundqvist B, Lambert G, Jensen G, Friberg P. Reduced spontaneous baroreceptor sensitivity in patients with renovascular hypertension. J Hypertens 2002; 20: 111-6.
42. Mussalo H, Vanninen E, Ikäheimo R, *et al.* Baroreflex sensitivity in essential and secondary hypertension. Clin Auton Res 2002; 12: 465-71.
43. Nishihara M, Hirooka Y, Matsukawa R. Kishi T, Sunagawa K. Oxidative stress in the rostral ventrolateral medulla modulates excitatory and inhibitory inputs in spontaneously hypertensive rats. J Hypertens 2012; 30: 97-106.

Original Article

Dietary Cholesterol Oxidation Products Accelerate Plaque Destabilization and Rupture Associated with Monocyte Infiltration/Activation via the MCP-1-CCR2 Pathway in Mouse Brachiocephalic Arteries: Therapeutic Effects of Ezetimibe

Kei Sato[1], Kaku Nakano[1], Shunsuke Katsuki[1], Tetsuya Matoba[1], Kyoichi Osada[2], Tatsuya Sawamura[3], Kenji Sunagawa[1] and Kensuke Egashira[1]

[1]Department of Cardiovascular Medicine, Graduate School of Medical Sciences, Kyushu University, Fukuoka, Japan
[2]Department of Agricultural Chemistry, Meiji University, Kanagawa, Japan
[3]Department of Vascular Physiology, National Cerebral and Cardiovascular Center Research Institute, Suita, Osaka, Japan

Aim: No prior studies have investigated the effects of dietary cholesterol oxidation products (oxysterols) on atherosclerotic plaque destabilization and rupture. We used an atherosclerotic mouse model with histological features similar to those seen in ruptured human plaques to test the hypothesis that (1) dietary oxysterols accelerate plaque destabilization and rupture and (2) a NPC1L1 inhibitor, ezetimibe, has therapeutic effects on these processes.

Methods and Results: Advanced atherosclerotic plaques were examined in innominate arteries of ApoE$^{-/-}$ mice that were fed either a regular high-fat diet (HFD) or HFD containing oxysterols (oxysterol-HFD; 6.8% of added cholesterol was oxidized) and infused with angiotensin II. Compared with HFD, oxysterol-HFD did not affect plasma lipid levels but did accelerate plaque destabilization and rupture, which was associated with increased monocyte infiltration/activation, monocyte chemoattractant protein-1 (MCP-1) expression, and matrix metalloproteinase (MMP) activity. Dietary oxysterol-induced plaque destabilization and rupture were blunted in ApoE$^{-/-}$CCR2$^{-/-}$ mice. Oral treatment with ezetimibe, significantly decreased plasma lipid levels and prevented the acceleration of plaque destabilization and rupture induced by dietary oxysterol. These data indicate a primary role for monocyte-mediated inflammation via the MCP-1-CCR2 pathway and the resultant increase in MMP activity in plaque destabilization and rupture induced by dietary oxysterols in ApoE$^{-/-}$ mice. These data also provide a mechanism by which dietary oxysterols are connected with the pathogenesis of plaque destabilization and rupture.

Conclusions: These data suggest that inhibition of the absorption of oxysterols by ezetimibe may be useful for the treatment of high-risk patients with high oxysterol intake.

J Atheroscler Thromb, 2012; 19:986-998.

Key words; Cholesterol oxidation products, Matrix metalloproteinase, Monocyte chemoattractant protein-1, Inflammation

Introduction

There is strong evidence that oxidized lipoproteins are atherogenic and play a key role in the pathogenesis of atherosclerotic vascular diseases[1-3]. Low-density lipoprotein (LDL) and other lipoproteins can be oxidized in atherosclerotic lesions or in the circulation[1-3]. Recent studies have raised the possibility that the levels of cholesterol oxidation products (oxysterols) in the diet may also be a risk factor for atherosclerosis and related vascular diseases. Oxysterols are known to be generated in food containing cholesterol (e.g., meats, eggs, and butter) by processing, cooking (deep-

Address for correspondence: Kensuke Egashira, Department of Cardiovascular Medicine, Graduate School of Medical Science, Kyushu University, 3-1-1, Maidashi, Higashi-ku, Fukuoka 812-8582, Japan
E-mail: egashira@cardiol.med.kyushu-u.ac.jp
Received: February 7, 2012
Accepted for publication: May 10, 2012

frying/heating) or prolonged storage in the presence of oxygen from the air[4]; therefore, relatively high levels of oxysterols (5-10% of the cholesterol content is oxidized) are found in typical cholesterol-rich Western diets, such as in fast foods[5]. Studies in animals and humans have reported that oxysterols from the diet are absorbed by the small intestine, incorporated into chylomicrons and LDL[6], and detected at higher levels in atherosclerotic lesions than in the circulation[7]. Staprans *et al.*[8, 9] have shown that the addition of oxysterols to the diet increases the severity of fatty streak lesions in the aorta in mouse and rabbit models of atherosclerosis.

Atherosclerotic plaque destabilization and rupture with vascular occlusive thrombosis is the most common cause of myocardial infarction in humans[2, 3, 10, 11], and non-occlusive plaque rupture may stimulate the progression of arterial stenosis; however, the molecular and cellular mechanisms behind plaque rupture remain poorly understood. Acquisition of a mechanistic understanding of plaque rupture could lead to the development of drugs that prevent or delay plaque rupture. Investigation of the mechanisms underlying the development of aortic atherosclerosis in animals may not necessarily reveal the mechanistic link to plaque destabilization and rupture because aortic atherosclerotic lesions in many animal models do not progress to plaque rupture spontaneously. No prior studies have investigated whether dietary oxysterols enhance plaque destabilization and rupture.

Ezetimibe, an inhibitor of the cholesterol transporter Niemann-Pick C1 Like 1 (NPC1L1) protein[12], inhibits the absorption of both dietary cholesterol and oxysterols in animals and humans[13], and thereby the development of aortic atherosclerosis induced by a regular Western diet containing pure cholesterol in animals[14, 15]. Prior studies, however, have not addressed the therapeutic effects of ezetimibe on atherosclerotic plaque development, destabilization and rupture induced by dietary oxysterols.

In the present study, we tested the hypothesis that dietary oxysterols accelerate atherosclerotic plaque destabilization and rupture. To test this hypothesis, we analyzed advanced brachiocephalic artery plaques in $ApoE^{-/-}$ mice that have histological features similar to those in ruptured human plaques[16-20]. To elucidate the mechanism behind dietary oxysterol-induced plaque destabilization and rupture, we performed mechanistic analyses of the plaques and documented that dietary oxysterols enhance monocyte infiltration/activation and MMP activity via the MCP-1-CCR2 pathway. We also tested the hypothesis that reducing the absorption of oxysterols by treatment with ezetimibe inhibits the oxysterol-induced increase in plaque destabilization and rupture.

Materials and Methods

Ethics Statement

The study protocol was reviewed and approved by the Committee on the Ethics of Animal Experiments, Kyushu University Graduate School of Medical Sciences. This investigation conforms with the Guide for the Care and Use of Laboratory Animals published by the US National Institutes of Health (NIH Publication No. 85-23, revised 1996). Blood collection and euthanasia were carried out by cervical dislocation after anesthesia with ketamine/xylazine (50 mg/kg and 1 mg/kg). Depth of anesthesia was monitored by the toe pinch reflex test.

Experimental Animals

Male $Apo\text{-}E^{-/-}$ mice with a C57BL/6J genetic background were purchased from Jackson Laboratory (Bar Harbor, ME)[21]. $ApoE^{-/-}CCR2^{-/-}$ double knockout mice with the same genetic background (C57BL/6J and 129/svjae hybrids) were used[22]. Animals were maintained on a 12 h light-dark cycle with free access to normal rodent chow and water.

Preparation of Oxysterol and Test Diet

Cholesterol auto-oxidation products (oxysterols) for the test diets were prepared from pure cholesterol (Riken Vitamin) by heating, as previously described[23]. In brief, cholesterol powder was placed on a cooking plate that was placed in a 200℃ gas oven and heated for 2 to 4 hours twice. The contents of the plate were re-dissolved in ether, and the composition of cholesterol oxidation products was analyzed by gas-liquid chromatography[23]. The following oxysterol products were present in the following amounts by weight percentage: cholesterol, 68; 7α-hydroxycholesterol, 3.7; 7β-hydroxycholesterol, 4.3; 5β-epoxycholesterol, 3.9; 5α-epoxycholesterol, 0.5; cholestanetriol, 1.6; 7-ketocholesterol, 4.4; and identified oxysterols, 13. Unidentified oxysterols comprised more than ten unknown peaks.

A high-fat diet (HFD) containing 21% fat from lard and supplemented with 0.15% (wt/wt) pure cholesterol (Oriental Yeast) was prepared according to the formula recommended by the American Institute of Nutrition. The diet contained the following constituents: casein, cystine, corn starch, sucrose, cholic acid, mineral mixture, vitamin mixture, powdered cellulose, choline bitartrate, and tert-butylhydroquinone.

In addition, an HFD containing oxysterols (oxy-

sterol-HFD) was prepared by adding oxysterols to the HFD at the expense of cholesterol. The oxysterol-HFD was identical to the HFD except that 6.8% of the added cholesterol consisted of oxysterols. Both HFD and oxysterol-HFD were stored at 4℃ to prevent the auto-oxidation of cholesterol.

Experimental Protocol

Starting at 18 weeks of age, ApoE$^{-/-}$ mice were divided into 2 groups, one to receive HFD, the other oxysterol-HFD. After 4 weeks on the experimental diets, all mice received angiotensin II (1.9 mg/kg per day) for 4 weeks[22, 24]. Angiotensin II was dissolved in phosphate-buffered saline and loaded into mini-osmotic pumps (Alzet, Cupertino, CA) according to the recommendations of the manufacturer. These pumps, containing angiotensin II, were placed intraperitoneally via a mid-scapular incision in mice under deep anesthesia with ketamine/xylazine (50 mg/kg and 1 mg/kg), the latter administered intraperitoneally.

At the start of the angiotensin II infusion, the HFD- and oxysterol-HFD-fed groups were further divided into the following four sub-groups: (1) control HFD-vehicle group that received oral administration of 0.5% carboxy methyl cellulose and (2) control HFD treated with ezetimibe group that was treated orally with ezetimibe at 5 mg/kg per day dissolved in 0.5% carboxy methyl cellulose for 4 weeks. (3) oxysterol HFD-vehicle group (4) oxysterol HFD treated with ezetimibe group. The dose of ezetimibe used in this study was selected because of the effectiveness reported in prior studies[14, 15]. Systolic blood pressure and heart rate were measured by the tail-cuff method before and 4 weeks after angiotensin II infusion.

Blood samples were collected for analysis from the left ventricle 1 or 4 weeks after angiotensin II infusion. Brachiocephalic arteries were isolated with a piece of the aortic arch and fixed in 10% buffered formalin for histological and immunohistochemical analyses.

Histopathology, Plaque Morphometry, and Immunohistochemistry

Brachiocephalic arteries were embedded in paraffin. Six sets of serial sections obtained at 30 μm intervals (starting from the proximal end of brachiocephalic artery) were stained with hematoxylin-eosin (HE) or Elastica van Gieson (EVG) to measure the incidence of plaque rupture, fibrous cap thickness and lipid core area, as previously described[16-19]. The average of the 6 images was reported for each animal. Moreover, serial brachiocephalic arterial sections were deparaffinized, and endogenous peroxidase was blocked by incubation with 0.3% H_2O_2 in methanol for 10 minutes. For antigen retrieval, sections were boiled for 20 minutes in citrate buffer (pH 6.0). After blocking with 3% skim milk, sections were incubated overnight at 4℃ with the anti-mouse macrophage antibody (Mac-3; dilution 1:100; Santa Cruz Biotechnology, Santa Cruz, CA) and anti-mouse MCP-1 antibody (dilution 1:200; Santa Cruz Biotechnology) followed by incubation with biotin-conjugated secondary antibodies. The sections were then washed and treated with avidin-biotin-peroxidase complexes. The sections were incubated with diaminobenzidine (DAB; Wako Pure Chemical, Osaka, Japan), and the nuclei were counterstained with hematoxylin.

Fibrous cap thickness was determined at the thinnest part of the cap by computerized image analysis. Plaque lipid core area was determined by digitally processing color images of HE-stained sections into monochrome, causing the tissue to be rendered as black and delipidated areas to appear as white. The total white area in the plaque was expressed as a percentage of the total plaque area to give the fractional lipid content. The Mac-3- and MCP-1-positive areas in atherosclerotic plaque were measured.

In the other sets of experiments, brachiocephalic arteries were embedded in OCT compound (Sakura Finetech) and subjected to cryosectioning (6 μm) using 7-KC and ApoB48 immunostaining and *in situ* zymography. 7-KC immunohistochemistry was performed using a Histofine mouse stain kit (Nichirei Biosciences). Sections were incubated with the anti-mouse 7-ketocholesterol antibody (dilution 1:100; Nikken Seil Corporation, Fukuroi, Japan). For apolipoprotein B48 immunostaining, the frozen sections were incubated with 0.3% H_2O_2 in PBS for 10 minutes to inhibit endogenous peroxidase activity. After blocking with 3% skim milk, sections were incubated overnight at 4℃ with HUC 20 IgY, which recognizes mouse ApoB48[25], followed by incubation with peroxidase-conjugated goat anti-chicken IgG (KPL). The 7-KC- and ApoB48-positive areas in atherosclerotic plaque were measured.

A single observer who was blinded to the experimental protocol performed quantitative analysis. All images were captured with a Nikon microscope equipped with a digital camera (HC-2500) and were analyzed using Adobe Photoshop 6.0 (Adobe Systems) and Scion Image 1.62 for Windows (Scion) software.

***In Situ* Zymography**

Gelatinase (MMP-2/gelatinase-A and MMP-9/gelatinase-B) activity was measured in unfixed frozen sections (6 μm thick) using quenched fluorescein-

labeled gelatinase substrate (DQ gelatin; Invitrogen)[26]. The fluorescent area produced by proteolytic digestion of quenched fluorescein-labeled gelatin was recognized as combined gelatinase activity (MMP-2 + MMP-9). The brachiocephalic artery sections were incubated at 37℃ for 30 minutes according to the manufacturer's protocol. Fluorescent microscopy (Olympus BX50) was used to detect gelatinase activity as green fluorescence. Negative control zymograms were incubated in the presence of 5 mM EDTA. The specific removal of essential divalent cations resulted in no detectable gelatinolytic activity.

Measurement of Blood Lipoprotein Profiles and Oxidative Stress

Serum total cholesterol and lipoprotein profiles (chylomicron, LDL-cholesterol, HDL-cholesterol and VLDL-cholesterol) were measured using an HPLC system with two tandem gel-permeation columns (Skylight Biotech, Akita, Japan)[27].

To measure serum oxidized LDL levels, serum levels of lectin-like oxidized LDL receptor-1 (LOX-1) ligand were determined using a sandwich enzyme-linked immunosorbent assay (ELISA), as described previously[28]. Serum LOX-1 ligand concentration was normalized to serum total cholesterol concentration (Cholesterol E-test; Wako Pure Chemical). Plasma concentrations of thiobarbituric acid reactive substances (TBARs) were determined as previously described[29].

Flowcytometry

Peripheral blood was drawn via cardiac puncture, and red blood cells were lysed with VersaLyse lysing solution (Becton Dickinson Biosciences, Franklin Lakes, NJ, USA) for 10 minutes at room temperature. Cells were incubated with a cocktail of mAb against CD115-PE (BD Pharmingen), CD11b-APC (BD Pharmingen) and Ly-6C-FITC (eBioscience) or appropriate isotype controls (BD Pharmingen) for 30 minutes at 4℃, followed by blocking Fc Receptor with anti-CD 16/32 mAb (BD Pharmingen) for 5 minutes at 4℃, and analyzed on a FACSCalibur (Becton Dickinson Biosciences). Monocyte subsets were identified as either Ly-6C^{hi} CD11b^{hi} CD115^{hi} or Ly-6C^{lo} CD11b^{hi} CD115^{hi}, as previously described[30].

Identification of Oxysterols in the Plasma and Liver

Gas-liquid chromatography mass spectrometry (GCMS-QP5050A mass spectrometer and GC-17 gas chromatograph; Shimazu) was performed to measure oxysterol levels in the plasma and liver[23]. Measurement conditions were as follows: a fused silica capillary ULBON HR-1 column (0.25 mm × 50 m) with a liquid-phase thickness of 0.25 mm; oven temperature, 270℃; injector temperature, 300℃; flow rate of helium, 0.7 mL/min; split ratio 1:50; make-up gas (helium), 40.1 mL/min. The mass spectra were measured within a mass range of m/z 50-600. The scan speed was one scan per second. The ionization energy was 70 eV.

Experimental Protocol using ApoE$^{-/-}$CCR2$^{-/-}$ Double Knockout Mice

To determine the primary role of oxysterol-mediated inflammation via MCP-1-CCR2 pathway in plaque destabilization and rupture, ApoE$^{-/-}$CCR2$^{-/-}$ mice were divided into 2 groups, one to receive HFD and the other oxysterol-HFD, as in the above experimental protocol, to examine the characteristics of brachiocephalic arteries, the lipid profile and flow cytometry.

Statistical Analysis

Data are expressed as the mean ± SEM. Data were analyzed using the Prism software program (GraphPad Software). Statistical analysis was assessed by two-way analysis of variance (ANOVA) followed by Bonferroni's post-hoc multiple comparison tests. Statistical comparison between two groups was evaluated by unpaired-t test. $P<0.05$ was considered significant.

Results

Serum Lipid Levels

There were no significant changes in serum cholesterol and other lipid parameters between Apo-E$^{-/-}$ mice fed an HFD and those fed an oxysterol-HFD (**Table 1**). Treatment with ezetimibe significantly decreased total serum cholesterol, chylomicron, VLDL cholesterol, and LDL cholesterol levels and increased HDL cholesterol levels.

No significant changes in serum oxidized LDL/cholesterol levels were observed between the HFD and oxysterol-HFD-fed groups (**Table 1**). Treatment with ezetimibe had no effect on serum oxidized LDL/cholesterol levels (**Table 1**).

There was no significant difference in body weight, heart rate or systolic blood pressure at weeks 0, 4, and 8 among the 4 groups (**Table 2**). Systolic blood pressure increased after angiotensin II infusion (week 8).

Plasma Lipid Peroxides

To examine whether oxysterol-HFD increases systemic oxidative stress, plasma lipid peroxide levels were measured (**Table 3**). There was no significant difference in lipid peroxide levels between the HFD and

Table 1. Serum lipid parameters and oxidized LDL (LOX-1 ligand) levels at week 8

	HFD		Oxysterol-HFD	
	Vehicle	Ezetimibe	Vehicle	Ezetimibe
Total Cholesterol (mg/dL)	678 ± 43 (n=11)	294 ± 12* (n=11)	706 ± 42 (n=12)	265 ± 16* (n=11)
Chylomicron (mg/dL)	93 ± 9 (n=6)	18 ± 1* (n=6)	84 ± 16 (n=7)	13 ± 1* (n=6)
VLDL-Cholesterol (mg/dL)	311 ± 17 (n=6)	105 ± 8* (n=6)	347 ± 24 (n=7)	84 ± 10* (n=6)
LDL-Cholesterol (mg/dL)	205 ± 16 (n=6)	122 ± 9* (n=6)	242 ± 8 (n=7)	118 ± 13* (n=6)
Oxidized LDL (LOX-1 ligand) (μg/dL)	151 ± 49 (n=7)	63 ± 14* (n=5)	129 ± 14 (n=9)	45 ± 9* (n=6)
Ratio of μg oxidized LDL (LOX-1 ligand) /mg cholesterol	0.20 ± 0.06 (n=7)	0.20 ± 0.04 (n=5)	0.19 ± 0.04 (n=9)	0.15 ± 0.03 (n=6)

Data are expressed as the mean ± SEM. Data were compared using two-way ANOVA followed by Bonferroni's multiple comparison tests. *$p<0.05$. versus vehicle. #$p<0.05$ versus vehicle in the HFD-fed group. CM, chylomicron; VLDL, very low-density lipoprotein; LDL, low-density lipoprotein; HDL, high-density lipoprotein.

Table 2. Body weight, heart rate and systolic blood pressure

	Weeks	HFD		Oxysterol-HFD	
		Vehicle	Ezeimibe	Vehicle	Ezeimibe
Body weight (g)	0	30.5 ± 0.7	31.2 ± 0.7	30.9 ± 0.7	31.2 ± 0.8
	4	31.9 ± 0.5	33.0 ± 0.5	33.0 ± 0.7	32.4 ± 0.7
	8	32.8 ± 0.6	33.3 ± 0.6	33.1 ± 0.9	33.3 ± 1.2
Heart Rate (beat/min)	0	561 ± 12	554 ± 18	573 ± 24	540 ± 16
	4	571 ± 13	571 ± 32	548 ± 20	518 ± 25
	8	609 ± 18	580 ± 16	605 ± 21	544 ± 32
Systolic Blood Pressure (mmHg)	0	112 ± 3	109 ± 3	110 ± 3	109 ± 3
	4	118 ± 3	116 ± 1	115 ± 3	113 ± 4
	8	137 ± 4*	134 ± 5*	130 ± 3*	131 ± 4*

Data are expressed as the mean ± SEM (n=5 to 9). *$p<0.05$ versus week 0.

Table 3. Plasma lipid peroxide levels

Weeks	unit	HFD		Oxysterol-HFD	
		Vehicle	Ezetimibe	Vehicle	Ezetimibe
Week 4 (before angiotensin II infusion)	μM	1.43 ± 0.07	–	1.56 ± 0.07	–
Week 5 (1 week after angiotensin II infusion)	μM	2.63 ± 0.53*	1.54 ± 0.18†	3.28 ± 0.59*#	1.66 ± 0.54†
Week 8 (4 week after angiotensin II infusion)	μM	2.58 ± 0.12*	2.04 ± 0.11	2.93 ± 0.21*	2.26 ± 0.16†

Data are expressed as the mean ± SEM (n=5 to 9). Data were compared using two-way ANOVA followed by Bonferroni's multiple comparison tests. *$p<0.05$ versus week 4. †$p<0.05$ versus vehicle. #$p<0.05$ versus vehicle in the HFD-fed group. Peroxide levels were determined by biochemical assays for thiobarbituric acid reactive substances (TBARs).

Table 4. Oxysterol Levels in the liver at week 8

μg/g tissue	HFD		Oxysterol-HFD	
	Vehicle ($n=3$)	Ezetimibe ($n=3$)	Vehicle ($n=5$)	Ezetimibe ($n=3$)
7α-hydroxy Cholesterol	1±0	2±2	5±1	3±1
7β-hydroxy Cholesterol	5±2	3±0	5±1	3±1
5α-epoxy Cholesterol	2±0	1±0	1±0	1±0
5β-epoxy Cholesterol	7±1	1±0	59±28	11±4
6-keto Cholesterol	1±0	0	1±0	0
7-keto Cholesterol	1±0	0	0	0
Total Oxysterols	17±2	7±1	72±29	17±5
Unknown Oxysterols	39±9	34±5	63±13	52±33
Cholesterol	15,407±4,389	9,242±695	10,888±3,476	6,409±1,143
Ratio of mg total oxysterols to g cholesterol	1.34±0.50	0.74±0.04	6.07±1.13#	2.55±0.40*

Data are expressed as the mean ± SEM. Data were compared using two-way ANOVA followed by Bonferroni's multiple comparison tests. *$p<0.05$ versus vehicle in the oxysterol-HFD-fed group. #$p<0.05$ versus vehicle in the HFD-fed group.

Table 5. Plasma oxysterol levels at week 8

μg/mL serum	HFD		Oxysterol-HFD	
	Vehicle	Ezetimibe	Vehicle	Ezetimibe
7α-hydroxy Cholesterol	2±2	1±1	2±2	2±1
7β-hydroxy Cholesterol	13±4	7±2	30±14	11±3
5α-epoxy Cholesterol	0	0	0	0
5β-epoxy Cholesterol	0	0	0	0
6-keto Cholesterol	0	0	0	0
7-keto Cholesterol	0	0	0	0
Total oxysterols	16±6	9±3	33±15	14±4
Unknown Oxysterols	1,558±1,264	111±104	1,852±1,320	5±1
Cholesterol	1,014±244	451±93	1,508±479	572±68
Ratio of mg total oxysterols to g cholesterol	9±6	13±4	10±4	27±11

Data are expressed as the mean ± SEM ($n=5$). Data were compared using two-way ANOVA followed by Bonferroni's multiple comparison tests.

Table 6. Histopathological and immunohistochemical analysis of brachiocephalic artery plaques at week 8

groups	HFD		Oxysterol-HFD	
	Vehicle ($n=12$)	Ezetimibe ($n=10$)	Vehicle ($n=13$)	Ezetimibe ($n=12$)
Histopathological findings				
Plaque Area ($\times10^4$ μm^2)	13.6±1.2	13.9±1.4	18.6±1.4#	13.9±1.6
Fibrous Cap Thickness (μm)	1.2±0.2	2.4±0.3*	1.1±0.1	2.3±0.3*
Lipid Core Area ($\times10^4$ μm^2)	2.1±0.4	2.4±0.6	4.6±0.7#	1.9±0.5*
Immunohistochemical findings				
Mac-3-positive Area ($\times10^4$ μm^2)	3.6±0.2	2.0±0.3	6.6±0.9#	3.6±0.2*
MCP-1-positive Area ($\times10^4$ μm^2)	3.9±0.4	1.7±0.3*	5.9±0.7#	3.0±0.3*

Data are expressed as the mean ± SEM. *$p<0.05$ versus vehicle group fed with HFD or oxysterol-HFD. #$p<0.05$ versus vehicle in the HFD-fed group. Data were compared using two-way ANOVA followed by Bonferroni's multiple comparison tests.

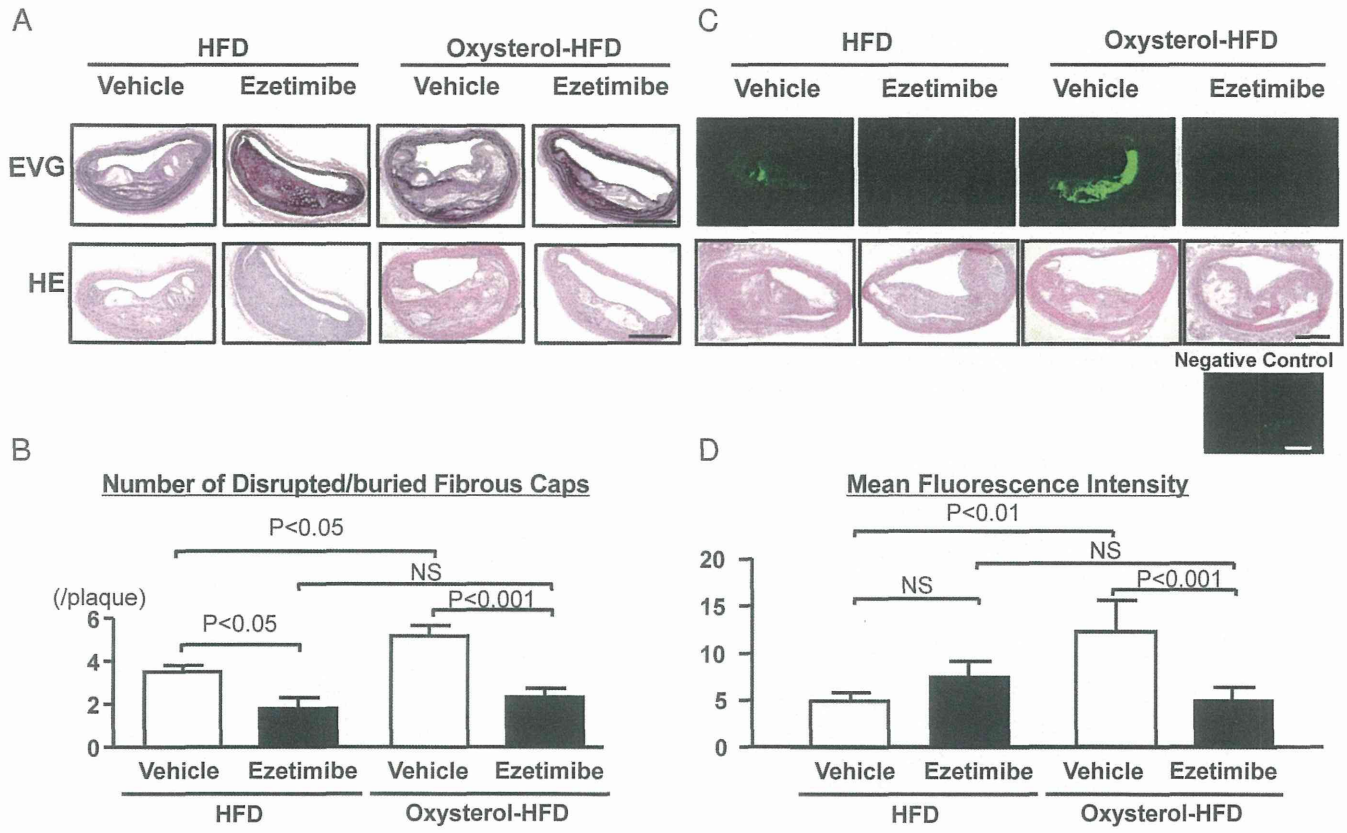

Fig. 1. Atherosclerotic plaque rupture in the brachiocephalic arteries of ApoE$^{-/-}$ mice. A, Photomicrographs of brachiocephalic artery plaques stained with Elastica van Gieson (EVG) or hematoxylin and eosin (HE). Bar indicates 100 μm. B, Quantitative comparison of the number of disrupted/buried fibrous caps. Data are indicated as mean ± SEM (n=10 to 13). C, In situ zymography of activated gelatinase in brachiocephalic artery plaques in ApoE$^{-/-}$ mice. C, Upper panels: fluorescence microscopy photomicrographs (green fluorescence indicates gelatinase activity). Negative control zymograms of the oxysterol-HFD-fed group were incubated in the presence of 1 mM EDTA. D, Lower panels: photomicrographs of serial sections stained with HE. Bar indicates 100 μm. D, Quantitative analysis of gelatinase activity. Data are reported as the mean ± SEM (n=6 to 9). Data were compared using 2-way ANOVA followed by Bonferroni's multiple comparison tests.

oxysterol-HFD-fed groups at week 4 (before Ang II infusion). At week 5 (1 week after Ang II infusion), plasma lipid peroxide levels were greater in the oxysterol-HFD-fed group than in the HFD-fed group. This difference became insignificant at week 8 (4 weeks after Ang II infusion). Treatment with ezetimibe significantly reduced lipid peroxide levels in both the HFD- and oxysterol-HFD-fed groups.

Oxysterol Levels in Plasma and Liver

Total oxysterol concentrations tended to increase in the livers of mice in the oxysterol-HFD-fed group compared to those in the HFD-fed group (**Table 4**). When the ratio of total oxysterols to cholesterol was examined, the ratio was higher in the oxysterol-HFD-fed group than in the HFD-fed group. Treatment with ezetimibe inhibited such an increase in the total oxysterol/cholesterol ratio. No significant changes were observed in plasma oxysterol levels among the 4 groups (**Table 5**).

Atherosclerotic Plaque Destabilization and Rupture in the Brachiocephalic Artery

Histopathological and immunohistochemical analyses of plaques in the brachiocephalic artery were performed to examine atherosclerotic plaque destabilization markers (lipid core area, fibrous cap thinning, and Mac-3-positive area) (**Table 6**). The presence of dietary oxysterols did not alter fibrous cap thickness but increased the lipid core area, mac-3-positive area, and plaque area. These changes in plaque destabilization markers were associated with increased MCP-1-positive areas. The number of disrupted/buried fibrous caps, a histopathological feature of plaque rupture, was then examined (**Fig. 1A** and **1B**). Feeding mice with oxysterol-HFD increased the incidence of plaque

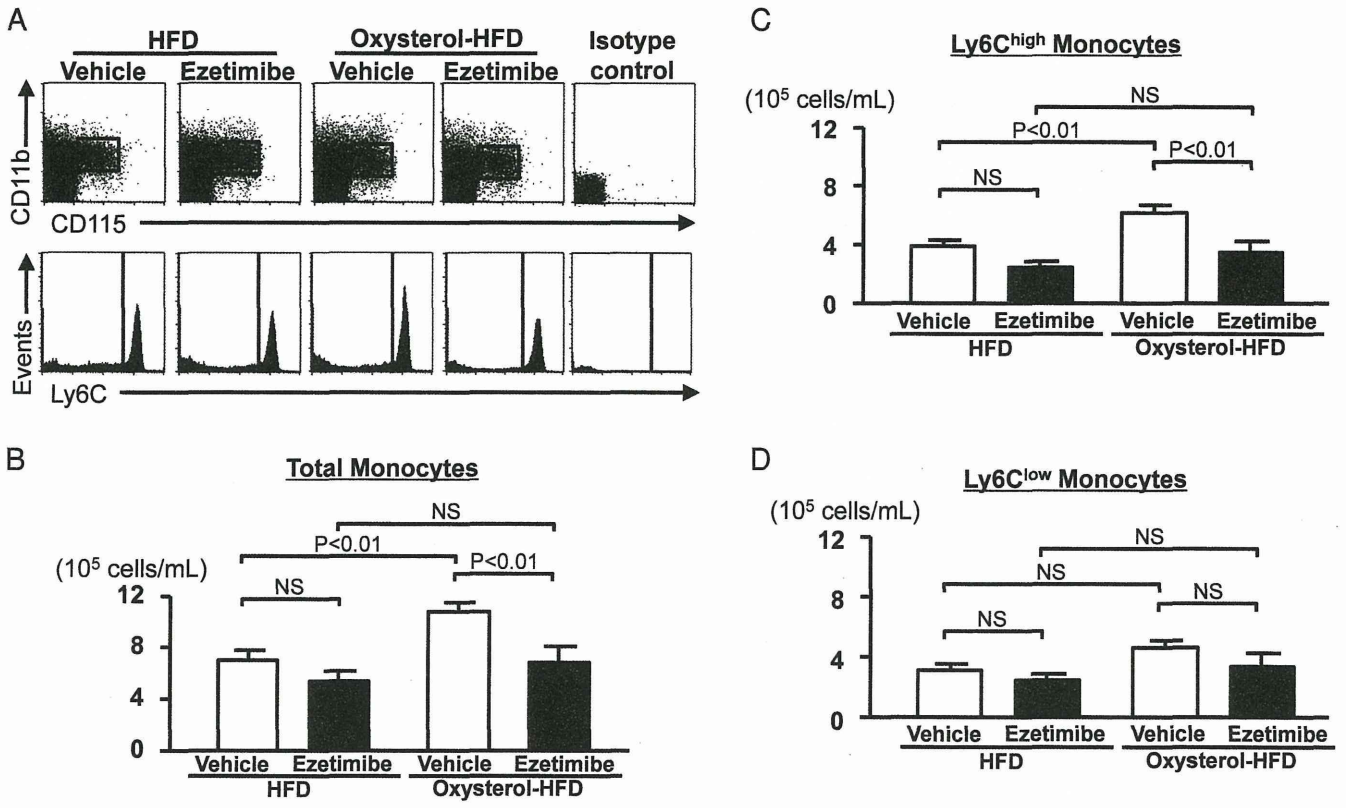

Fig. 2. Flow cytometric analysis of blood monocytes in ApoE$^{-/-}$ mice. A, Representative flow cytometry dot plots and histograms from ApoE$^{-/-}$ mice. The number of blood monocytes was determined by co-expression of CD115 and CD11b. Blood CD115^{+}CD11b^{+} monocytes were divided into Ly6C^{hi} and Ly6C^{lo} subsets. B, Total blood CD115^{+}CD11b^{+} monocytes. C, Total blood Ly6C^{hi}CD115^{+}CD11b^{+} monocytes. D, Total blood Ly6C^{lo}CD115^{+}CD11b^{+} monocytes. Data are reported as the mean ± SEM (n = 5 to 9). Data were compared using 2-way ANOVA followed by Bonferroni's multiple comparison tests.

rupture compared with the HFD-vehicle-fed group.

Treatment with ezetimibe prevented the oxysterol-HFD-induced increase in plaque destabilization markers (i.e., lipid core area, monocyte area, plaque size) and rupture. Treatment with ezetimibe also increased fibrous cap thickness in both the HFD- and oxysterol-HFD-fed groups.

In Situ Zymography

Analysis of gelatinase activity, reflecting the combined activity of MMP-2 and MMP-9, by *in situ* zymography showed enhanced gelatinase activity in areas of monocyte/macrophage infiltration. Treatment with ezetimibe inhibited increased gelatinase activity in the oxysterol-HFD-fed group (**Fig. 1C** and **1D**).

Flow Cytometric Analysis of Blood Monocyte Subsets

The monocyte Ly6C^{hi} subset is reported to play a critical role in atherosclerotic plaque progression in mice[30, 31]. Oxysterol-HFD feeding increased the number of circulating monocytes at week 8 (**Fig. 2**). This monocytosis was associated with an increase in Ly6C^{hi} subsets, but not with increases in Ly6C^{lo} subsets. Treatment with ezetimibe prevented monocytosis of the Ly6C^{hi} subsets induced by oxysterol-HFD.

Immunohistochemical Analysis of 7-Ketocholesterol and ApoB48

Immunohistochemical analysis showed the presence of 7-ketocholesterol (a representative oxysterol derived from diet) in brachiocephalic artery plaques (**Fig. 3**). Quantitative analysis revealed an increase in 7-ketocholesterol-positive areas in the oxysterol-HFD-fed group and treatment with ezetimibe inhibited this increase. Serial sections of brachiocephalic artery plaques were immunostained with antibodies for either 7-ketocholesterol or ApoB48 (a lipoprotein synthesized in the small intestine, incorporated into chylomicrons, and essential for intestinal lipid absorption) (**Fig. 3C**). Interestingly, 7-ketocholesterol-positive areas colocalized with ApoB48-positive areas.

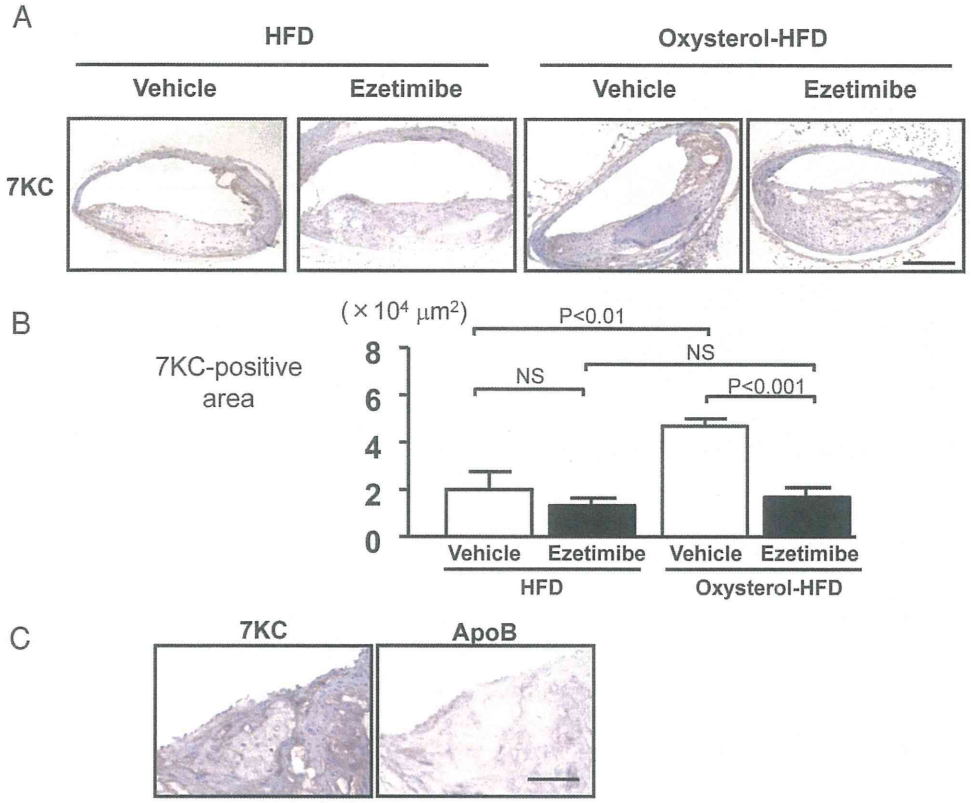

Fig. 3. Immunohistochemical analyses of 7-ketocholesterol (7KC) in the brachiocephalic arteries of ApoE$^{-/-}$ mice. A, Photomicrographs of brachiocephalic artery plaques stained with 7KC. Scale bar indicates 100 μm. B, Quantitative analysis of the 7KC-positive area. Data are reported as the mean ± SEM (n=4 to 6). Data were compared using 2-way ANOVA followed by Bonferroni's multiple comparison tests. C, Co-localization study: representative photographs of serial sections immunohistochemically stained with 7KC and ApoB. Scale bar indicates 50 μm.

Atherosclerotic Plaque Destabilization and Rupture in ApoE$^{-/-}$CCR2$^{-/-}$ Mice

To determine the role of the MCP-1-CCR2 pathway in atherosclerotic plaque rupture, ApoE$^{-/-}$CCR2$^{-/-}$ mice were used[22]. In ApoE$^{-/-}$CCR2$^{-/-}$ mice, oxysterol-HFD feeding did not induce plaque destabilization and rupture in brachiocephalic artery plaques (**Fig. 4A**, **4B** and **Table 7**). In addition, double-knockout mice did not display an increase in monocyte infiltration, MCP-1 expression, and systemic monocytosis of Ly6C^{hi} monocyte subsets at week 8 (**Fig. 4C** and **4D**). There was no difference in serum cholesterol levels between HFD and oxysterol-HFD groups (**Table 7**).

Discussion

Hyperlipidemic mice with advanced atherosclerotic brachiocephalic artery plaques appear to be a suitable animal model for elucidating the molecular and cellular mechanisms behind human plaque rupture. This model is used because, unlike other models of aortic atherosclerosis, brachiocephalic artery plaques represent several key histological features of ruptured human plaques, including an increase in plaque destabilization markers (monocyte infiltration/activation, lipid accumulation, fibrous cap thinning due to decreased smooth muscle content) and evidence of disrupted/buried fibrous caps[16-19]; however, this model has been criticized because it does not display other histological features of human plaque rupture including occlusive thrombosis[16-19], which is thought to be a reflection of differences in the coagulation and thrombolytic systems between the 2 species. In addition, the incidence of rupture in this original hyperlipidemic mouse model is too infrequent (10-20% without HFD feeding[18] and 40-60% per plaque after HFD feeding[17]) to allow for mechanistic examina-

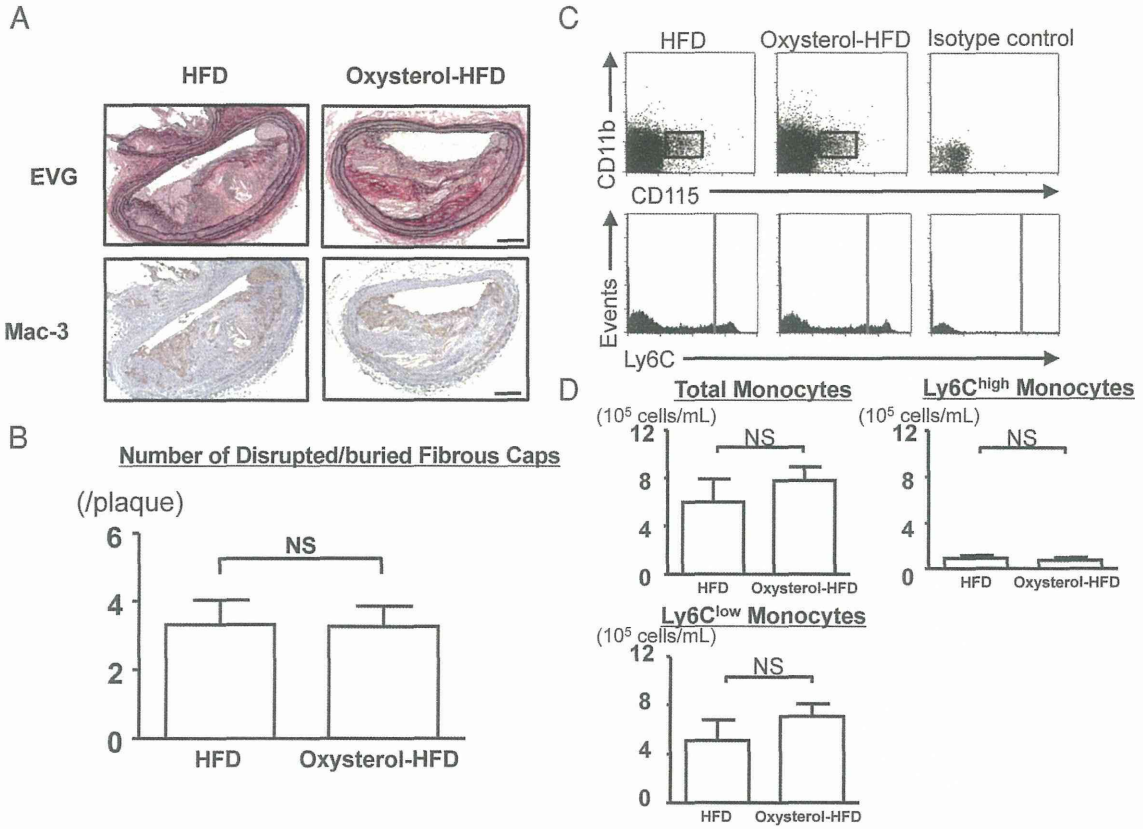

Fig. 4. Atherosclerotic plaque rupture in the brachiocephalic arteries of ApoE$^{-/-}$CCR2$^{-/-}$ mice. A, Photomicrographs of brachiocephalic artery plaques stained with EVG and immunostained with mac-3. B, Quantitative comparison of the number of disrupted/buried fibrous caps and the mac-3-positive area. Scale bar indicates 100 μm. $n=6$ to 7. C, Flow cytometric analysis of blood monocytes in ApoE$^{-/-}$ CCR2$^{-/-}$ mice. A, Representative flow cytometry dot plots and histograms of blood. D, The number of blood monocytes was determined by co-expression of CD115 and CD11b. Blood CD115^{+}CD11b^{+} monocytes were divided into Ly6C^{hi} and Ly6C^{lo} subsets. Data are reported as the mean ± SEM ($n=6$ to 9). Data are compared using the unpaired-t test.

tions and analysis of the effects of new modalities that inhibit plaque destabilization and rupture. In a previous study that examined the therapeutic effects of anti-atherosclerotic drugs[17], an excess of 60 animals was needed per group to ensure that the studies were adequately powered. To overcome this problem, we performed chronic infusion of angiotensin II in addition to HFD feeding in ApoE$^{-/-}$ mice because this has been used to enhance the features of atherogenesis, such as monocyte-mediated inflammation, lipid accumulation, and MMP activation[22, 24]. We found that chronic angiotensin II infusion could increase the incidence of plaque rupture from less than 1 rupture per plaque (authors' unpublished observation) to 3.4 per plaque (**Fig. 1A** and **1B**); therefore, in the present study, we used this modified model to investigate whether dietary oxysterols accelerate plaque rupture and whether ezetimibe has therapeutic effects on atherosclerosis.

We report here for the first time that oxysterol-HFD feeding does not affect plasma lipid levels but enhances plaque destabilization and rupture. Mechanistic analyses of the plaques showed that oxysterol-HFD increased the infiltration of monocytes/macrophages, MCP-1 expression, and lipid core size in the plaques. Monocytosis associated with an increase in the Ly6c^{hi} monocyte subset in circulating blood was also noted in the oxysterol-HFD-fed group. Importantly, monocyte activation and other pathogenetic features seen in plaques in ApoE$^{-/-}$ mice fed oxysterol-HFD were blunted in ApoE$^{-/-}$CCR2$^{-/-}$ mice fed oxysterol-HFD. Accumulating evidence in humans and animals indicates that activated monocytes/macrophages play a key role in causing plaque destabilization and rupture by secreting MMP-9/gelatinase-B and MMP-2/gelatinase-A, which break down the

Table 7. Characteristics of brachiocephalic artery plaques, lipid profile and TBARS in ApoE$^{-/-}$ CCR2$^{-/-}$ mice at week 8

	HFD group	Oxysterol-HFD group
Plaque area ($\times 10^4$ μm^2)	28.1 ± 3.7 (n=6)	26.1 ± 6.3 (n=8)
Fibrous cap thickness (μm)	2.1 ± 0.2 (n=6)	1.9 ± 0.4 (n=8)
Lipid core area ($\times 10^4$ μm^2)	6.9 ± 2.0 (n=6)	5.6 ± 1.2 (n=8)
Mac-3-positive area ($\times 10^4$ μm^2)	4.5 ± 0.8 (n=6)	3.8 ± 0.7 (n=8)
MCP-1-positive area ($\times 10^4$ μm^2)	6.7 ± 1.4 (n=6)	4.3 ± 0.6 (n=8)
Serum cholesterol levels (mg/dL)	1,326 ± 80 (n=5)	1,207 ± 78 (n=8)
Plasma lipid peroxide (μM)	6.2 ± 0.4 (n=5)	6.3 ± 0.3 (n=8)

Data are expressed as the mean ± SEM.

extracellular matrix (a determinant of the integrity of fibrous caps)[3, 32]. Gough *et al.*[18] reported that macrophage-targeted expression of a constitutively active MMP-9 mutant resulted in increased incidence of plaque rupture in advanced brachiocephalic artery plaques of ApoE$^{-/-}$ mice. Clinical studies have shown a correlation between MMP-9 and MMP-2 and cardiovascular events in patients with acute coronary syndrome[33, 34]; therefore, we examined gelatinase activity using *in situ* zymography and found enhanced gelatinase activity in areas of inflammatory cell infiltration in the oxysterol-HFD-fed group. In *in vitro* experiments, addition of oxysterol (7-KC) to murine macrophages induced MCP-1 production but did not alter MMP secretion. The data from this study and an aforementioned study[18] are consistent with the idea that enhanced monocyte-mediated inflammation and the resulting increase in macrophage MMP activity can induce plaque destabilization and rupture.

Oxysterol measurements using gas-liquid chromatography mass spectrometry showed that dietary oxysterol intake resulted in an increase in liver oxysterol concentrations, but did not lead to an increase in plasma oxysterol concentrations. In contrast, immunohistochemical analysis showed an increase in oxysterols (7-KC) in monocyte-positive areas of the plaques, which was greater in the oxysterol-HFD-fed group than in the HFD-fed group. Interestingly, 7-KC appeared to co-localize with ApoB48 (a lipoprotein involved in lipid absorption in the small intestine). Because dietary oxysterols did not affect oxidized LDL/cholesterol ratios in the plasma, it is unlikely that oxysterols incorporated into LDL play a major role in the pathogenesis of plaque destabilization and rupture; therefore, these data suggest a major role for monocyte/macrophage accumulation of diet-derived oxysterols in causing plaque destabilization and rupture.

Another new finding of the present study was that treatment with ezetimibe prevented plaque destabilization and rupture induced by dietary oxysterols. It is likely that these observed therapeutic effects resulted largely from the lipid-lowering effects of ezetimibe, which markedly decreases LDL cholesterol, chylomicron, and VLDL cholesterol levels and increases HDL cholesterol levels, as reported in patients with dyslipidemia. Ezetimibe also inhibited oxysterol accumulation in the liver and plaques, monocyte infiltration/activation, and MMP activity. The latter therapeutic effects might not necessarily be totally explained by the lipid-lowering effects of ezetimibe treatment; rather, they may result partly from a unique effect of ezetimibe, such as inhibition of dietary oxysterol absorption in the small intestine and reduced accumulation of oxysterols in atherosclerotic plaques, which can prevent plaque destabilization and rupture. These data suggest that ezetimibe could be a new therapeutic modality for subjects who overindulge in oxysterol-rich Western food and in patients at high risk for cardiovascular disease owing to high plasma oxysterol levels. Because Western diets have become prevalent in non-Western countries in this era of global civilization, the quantity of oxysterols consumed in the diet is of clinically importance for the paradigm shift in the pathogenesis of atherosclerotic vascular diseases. These data indicate a primary role for monocyte infiltration/activation via the MCP-1-CCR2 pathway and the resultant increase in combined gelatinase activity (MMP-2 + MMP-9) in plaque destabilization and rupture induced by dietary oxysterols in this model. These data suggest a mechanism that connects dietary oxysterols with the pathogenesis of plaque destabilization and rupture. Our results also suggest that inhibiting the absorption of dietary oxysterols with ezetimibe may be a useful treatment for high-risk patients with increased dietary oxysterol intake or whose plasma oxysterol concentrations are elevated.

Acknowledgments

The authors declare that they have no competing financial interests. This study was supported by Grants-in-Aid for Scientific Research (22390160) from the Ministry of Education, Science, and Culture, Tokyo, Japan.

Conflicts of Interest

No.

References

1) Steinberg D. Lewis A: Conner memorial lecture. Oxidative modification of ldl and atherogenesis. Circulation, 1997; 95: 1062-1071
2) Libby P, Ridker PM, Maseri A: Inflammation and atherosclerosis. Circulation, 2002; 105: 1135-1143
3) Libby P, Aikawa M: Stabilization of atherosclerotic plaques: New mechanisms and clinical targets. Nat Med, 2002; 8: 1257-1262
4) Brown AJ, Jessup W: Oxysterols and atherosclerosis. Atherosclerosis, 1999; 142: 1-28
5) Carpenter KL: Good cop, bad cop: An unsolved murder. Are dietary cholesterol oxidation products guilty of atherogenicity? Br J Nutr, 2002; 88: 335-338
6) Staprans I, Pan XM, Rapp JH, Feingold KR: Oxidized cholesterol in the diet is a source of oxidized lipoproteins in human serum. J Lipid Res, 2003; 44: 705-715
7) Garcia-Cruset S, Carpenter KL, Guardiola F, Stein BK, Mitchinson MJ: Oxysterol profiles of normal human arteries, fatty streaks and advanced lesions. Free Radic Res, 2001; 35: 31-41
8) Staprans I, Pan XM, Rapp JH, Grunfeld C, Feingold KR: Oxidized cholesterol in the diet accelerates the development of atherosclerosis in ldl receptor- and apolipoprotein e-deficient mice. Arterioscler Thromb Vasc Biol, 2000; 20: 708-714
9) Staprans I, Pan XM, Rapp JH, Feingold KR: Oxidized cholesterol in the diet accelerates the development of aortic atherosclerosis in cholesterol-fed rabbits. Arterioscler Thromb Vasc Biol, 1998; 18: 977-983
10) Falk E, Shah PK, Fuster V: Coronary plaque disruption. Circulation, 1995; 92: 657-671
11) Gustafson B: Adipose tissue, inflammation and atherosclerosis. J Atheroscler Thromb, 2010; 17: 332-341
12) Altmann SW, Davis HR Jr, Zhu LJ, Yao X, Hoos LM, Tetzloff G, Iyer SP, Maguire M, Golovko A, Zeng M, Wang L, Murgolo N, Graziano MP: Niemann-pick c1 like 1 protein is critical for intestinal cholesterol absorption. Science, (New York, N.Y. 2004; 303: 1201-1204)
13) Staprans I, Pan XM, Rapp JH, Moser AH, Feingold KR: Ezetimibe inhibits the incorporation of dietary oxidized cholesterol into lipoproteins. J Lipid Res, 2006; 47: 2575-2580
14) Davis HR Jr, Compton DS, Hoos L, Tetzloff G: Ezetimibe, a potent cholesterol absorption inhibitor, inhibits the development of atherosclerosis in apoe knockout mice. Arterioscler Thromb Vasc Biol, 2001; 21: 2032-2038
15) Nakagami H, Osako MK, Takami Y, Hanayama R, Koriyama H, Mori M, Hayashi H, Shimizu H, Morishita R: Vascular protective effects of ezetimibe in apoe-deficient mice. Atherosclerosis, 2009; 203: 51-58
16) Rosenfeld ME, Polinsky P, Virmani R, Kauser K, Rubanyi G, Schwartz SM: Advanced atherosclerotic lesions in the innominate artery of the apoe knockout mouse. Arterioscler Thromb Vasc Biol, 2000; 20: 2587-2592
17) Johnson J, Carson K, Williams H, Karanam S, Newby A, Angelini G, George S, Jackson C: Plaque rupture after short periods of fat feeding in the apolipoprotein e-knockout mouse: Model characterization and effects of pravastatin treatment. Circulation, 2005; 111: 1422-1430
18) Gough PJ, Gomez IG, Wille PT, Raines EW: Macrophage expression of active mmp-9 induces acute plaque disruption in apoe-deficient mice. J Clin Invest, 2006; 116: 59-69
19) Clarke MC, Figg N, Maguire JJ, Davenport AP, Goddard M, Littlewood TD, Bennett MR: Apoptosis of vascular smooth muscle cells induces features of plaque vulnerability in atherosclerosis. Nat Med, 2006; 12: 1075-1080
20) Cicha I, Regler M, Urschel K, Goppelt-Struebe M, Daniel WG, Garlichs CD: Resveratrol inhibits monocytic cell chemotaxis to mcp-1 and prevents spontaneous endothelial cell migration through rho kinase-dependent mechanism. J Atheroscler Thromb, 2011; 18: 1031-1042
21) Zhang S, Wang X, Zhang L, Yang X, Pan J, Ren G: Characterization of monocyte chemoattractant proteins and cc chemokine receptor 2 expression during atherogenesis in apolipoprotein e-null mice. J Atheroscler Thromb, 2011; 18: 846-856
22) Ishibashi M, Egashira K, Zhao Q, Hiasa K, Ohtani K, Ihara Y, Charo IF, Kura S, Tsuzuki T, Takeshita A, Sunagawa K: Bone marrow-derived monocyte chemoattractant protein-1 receptor ccr2 is critical in angiotensin ii-induced acceleration of atherosclerosis and aneurysm formation in hypercholesterolemic mice. Arterioscler Thromb Vasc Biol, 2004; 24: e174-178
23) Osada K, Kodama T, Minehira K, Yamada K, Sugano M: Dietary protein modifies oxidized cholesterol-induced alterations of linoleic acid and cholesterol metabolism in rats. J Nutr, 1996; 126: 1635-1643
24) Ni W, Kitamoto S, Ishibashi M, Usui M, Inoue S, Hiasa K, Zhao Q, Nishida K, Takeshita A, Egashira K: Monocyte chemoattractant protein-1 is an essential inflammatory mediator in angiotensin ii-induced progression of established atherosclerosis in hypercholesterolemic mice. Arterioscler Thromb Vasc Biol, 2004; 24: 534-539
25) Sato Y, Nishimichi N, Nakano A, Takikawa K, Inoue N, Matsuda H, Sawamura T: Determination of lox-1-ligand activity in mouse plasma with a chicken monoclonal antibody for apob. Atherosclerosis, 2008; 200: 303-309
26) Satoh K, Nigro P, Matoba T, O'Dell MR, Cui Z, Shi X, Mohan A, Yan C, Abe J, Illig KA, Berk BC: Cyclophilin a enhances vascular oxidative stress and the development of angiotensin ii-induced aortic aneurysms. Nat Med, 2009; 15: 649-656
27) Usui S, Hara Y, Hosaki S, Okazaki M: A new on-line dual

enzymatic method for simultaneous quantification of cholesterol and triglycerides in lipoproteins by hplc. J Lipid Res, 2002; 43: 805-814
28) Ishigaki Y, Katagiri H, Gao J, Yamada T, Imai J, Uno K, Hasegawa Y, Kaneko K, Ogihara T, Ishihara H, Sato Y, Takikawa K, Nishimichi N, Matsuda H, Sawamura T, Oka Y: Impact of plasma oxidized low-density lipoprotein removal on atherosclerosis. Circulation, 2008; 118: 75-83
29) Yagi K: Assay for blood plasma or serum. Methods Enzymol, 1984; 105: 328-331
30) Swirski FK, Libby P, Aikawa E, Alcaide P, Luscinskas FW, Weissleder R, Pittet MJ: Ly-6chi monocytes dominate hypercholesterolemia-associated monocytosis and give rise to macrophages in atheromata. J Clin Invest, 2007; 117: 195-205
31) Tacke F, Alvarez D, Kaplan TJ, Jakubzick C, Spanbroek R, Llodra J, Garin A, Liu J, Mack M, van Rooijen N, Lira SA, Habenicht AJ, Randolph GJ: Monocyte subsets differentially employ ccr2, ccr5, and cx3cr1 to accumulate within atherosclerotic plaques. J Clin Invest, 2007; 117: 185-194
32) Crisby M, Nordin-Fredriksson G, Shah PK, Yano J, Zhu J, Nilsson J: Pravastatin treatment increases collagen content and decreases lipid content, inflammation, metalloproteinases, and cell death in human carotid plaques: Implications for plaque stabilization. Circulation, 2001; 103: 926-933
33) Kai H, Ikeda H, Yasukawa H, Kai M, Seki Y, Kuwahara F, Ueno T, Sugi K, Imaizumi T: Peripheral blood levels of matrix metalloproteases-2 and -9 are elevated in patients with acute coronary syndromes. J Am Coll Cardiol, 1998; 32: 368-372
34) Inokubo Y, Hanada H, Ishizaka H, Fukushi T, Kamada T, Okumura K: Plasma levels of matrix metalloproteinase-9 and tissue inhibitor of metalloproteinase-1 are increased in the coronary circulation in patients with acute coronary syndrome. Am Heart J, 2001; 141: 211-217